LA-UR -90-4351

Conf-901072--2

Received by OSTI

JAN 0 8 1991

LA-UR--90-4351

DE91 005750

TITLE. QCD WITH DYNAMICAL WILSON FERMIONS

AUTHOR(S): RAJAN GUPTA

SUBMITTED TO: NUCLEAR PHYSICS/PROCEEDINGS OF LATTICE'90 CONFERENCE HELD IN TALLAHASSEE, FL 10/7-12/90.

DISCLAIMER

MASTER

Los Alamos Los Alamos National Laboratory
Los Alamos, New Mexico 87545

FORM NO. 836 R4
ST NO 2629 5/91

QCD WITH DYNAMICAL WILSON FERMIONS

Rajan GUPTA

T8 MS-B285, Los Alamos National Lab., Los Alamos, NM 87545, USA
Institute of Theoretical Physics, UCSB, Santa Barbara, CA 93106, USA

In collaboration with C. Baillie, R. Brickner, G. Kilcup, A. Patel and S. Sharpe.

Results for the spectrum and the F and D parameters are obtained with precision similar to that in the quenched approximation. Present data for $m_q \geq m_s$ show measurable effects due to vacuum polarization only in the pion-Nucleon Σ term suggesting that $\Sigma^{sea} \sim \Sigma^{val}$. The lattice update is being done on the Connection Machine which is very well suited to simulate QCD with 2 flavors of Wilson fermions (with mass close to the strange quark) using HMCA on $16^3 \times 32$ lattices.

1. Introduction: In this talk I present the status of QCD simulations with $n_f = 2$ flavors of Wilson fermions being done on the Connection Machine (at Los Alamos, TMC, Argonne, Sandia and Syracuse) and Cray YMP (at LANL, SDSC and PSC). We are generating lattices using the Hybrid Monte Carlo Algorithm (HMCA) [1] [2] at $\beta = 5.4$, 5.5, and 5.6. At each of these three values of β we are simulating a number of values of κ. This exploration of parameter space is necessary in order to (a) study the effect of quark loops, (b) evaluate the behavior and efficacy of HMCA as the quark mass is reduced ($\kappa \to \kappa_c$), and (c) examine the scaling behavior of observables.

The details of the update are given in Table 1 and a longer writeup is under preparation. The performance of the QCD code on the CM2 has been described by R. Brickner at this conference [3]. Here I outline the method we use for tuning HMCA and give some data showing that the auto-correlation times in the update are large.

Part of our 16^4 lattices have the following error: the front-end random number generator (used only in the crucial Metropolis accept/reject step) was by default initialized with the same starting seed at the beginning of each restart of the job. Most of the time a run consisted of a few trajectories, so using the same sequence is expected to produce a bias. Table 1 gives the breakup of update runs with and without this bug. We have comparable data for the two cases and do not find a significant difference between them. The more significant limitation of the current results is poor statistics. It is our guess that errors due to the bias are less than the statistical errors. We are now updating $16^3 \times 32$ lattices at $\beta = 5.5, \kappa = 0.160$ and $\beta = 5.6, \kappa = 0.157$ and 0.1575. In due course this will provide an independent statistical sample for comparison and it will also allow us to extract effective masses at larger time separation.

β	κ_d	ϵ	N_{md}	N_{traj}^{old}	N_{traj}^{new}	A
5.4	.160	0.017	45; 20		600	−; 60%
5.4	.161	0.015	50; 20		1080	−; 61%
5.4	.162	0.010	70; 35	310		74; −%
5.4	.163	0.011	35; 20		160	−; 63%
5.5	.158	0.011	70; 30	320		60; −%
5.5	.159	0.010	70; 40	400		60; −%
5.5	.160	0.008	100; 40	400	135	62; 68%
5.6	.156	0.0145	50; 20	220	80	84; 65%
5.6	.157	0.0090	80; 40	440	200	63; 83%
5.6	.1575	0.008	50; 30		150	−; 79%

Table 1: Run Parameters for the lattices. The trajectories are of random length $N_{md} = a + b * ranf()$. The number of trajectories generated before (N_{traj}^{old}) and after (N_{traj}^{new}) fixing the bug are given separately along with the corresponding acceptance rates.

The new results presented here are for (a) the hadron spectrum and (b) the SU(3) symmetry breaking parameters F and D for the proton using scalar and axial density insertions. Results for the moments of the quark distribution amplitude for the pion were presented by D. Daniel [4]. All these results are obtained for quark masses in the range

$m_s < m_q < 3m_s$ for which we expect effects of vacuum polarization in physical observables to be small. Similarly, the weakest coupling used, $\beta = 5.6$, is perhaps just at the beginning of the scaling region. So, these exploratory first results lay down the guidelines for the parameter values at which future calculations should be done.

2. Tuning HMCA: In our previous studies of tuning ϵ we had analyzed data on 8^4 lattices (Wilson fermions) and up to 4×10^3 lattices (staggered) [5]. Our conclusion, for the version of leap frog algorithm in which the links are updated at the first half step, was that a 10-20 % gain in acceptance can be obtained provided one tunes $\beta - \beta_{MD} \approx 0.008$ and $m_{MD} - m \approx 0.001$. Our new tests on 16^4 lattices (Wilson) and $16^3 \times 24$ lattices (staggered) show that these shifts are too large and much better acceptance is obtained with $\beta = \beta_{MD}$ and $m = m_{MD}$ for both kinds of fermions. Since tuning affects the total action which is an extensive quantity, we conjecture that one needs to reduce the shifts in β and m given above by the ratio of lattice volumes.

A simple empirical method for tuning that does not require high statistics is as follows: on a given starting configuration monitor the change in the action at each step of the trajectory as a function of ϵ, β_{md} and κ_{md}. The goal is to reduce fluctuations in ΔS over the length of the trajectory to within the interval [-1,1]. Figure 1 shows the results of a test for 3 values of β_{md}. As advertised, of the three cases $\beta_{md} = \beta$ is the best. We have not yet made tests with smaller shifts.

3. Autocorrelations: We find that the lowest order implementation of HMCA exhibits long autocorrelation times. We have monitored the time history of hadron correlators along with up to 6×6 Wilson loops and find similar long auto-correlations in all observables. In Fig. 2 we show a typical time history for the pion correlator. On the basis of such correlations observed in time histories, we conclude that runs with HMCA exhibit autocorrelation times of at least a few hundred trajectories even though our present data sets are too short to determine these accurately. The time histories do not show any long time drifts in the observables. Nevertheless, we will continue to monitor the data to check if thermalization is complete since the present runs, measured in units of decorrelation times, are short. We typically discarded the first 200 time units for this purpose.

Fig 1: Variation of ΔS for $\beta - \beta_{md} = 0.008$ (o), $\beta_{md} = \beta$ (solid line) and $\beta_{md} - \beta = 0.005$ (dashed line) starting with the same thermalized lattice at $\beta = 5.6$, $\kappa = 0.157$ and with $\epsilon = 0.012$

Fig. 2: Time history of pion correlator at $\beta = 5.5$ and $\kappa = 0.160$ at time separations 9 ($\times$), 10 (o) and 11 (+).

4. The Lattice Scale, κ_c and κ_s: We define $\kappa_c(g)$ using a linear extrapolation for m_π^2 in $1/\kappa$ keeping $\kappa^u = \kappa^d = \kappa$. The lattice scale a^{-1} for a given β is determined by setting the ρ mass at κ_c to 770 MeV. To compare against quenched calculations we estimate β^a_{eff}, the equivalent gauge coupling for the quenched theory which has the same scale, and β^κ_{eff}, the quenched gauge coupling which has the same κ_c. These parameters are listed in Table 2. If β^κ_{eff} and β^a_{eff} agree then the effect of dynamical fermions might be regarded as a simple renormalization of the pure gauge coupling. Our present data show that this is not the case.

For $r = 1$ Wilson fermions, the quark mass is defined by $m_q a = \log\left(1 + 0.5(\frac{1}{\kappa} - \frac{1}{\kappa_c})\right)$, however, the naive mass term in the action is $0.5(\frac{1}{\kappa} - \frac{1}{\kappa_c})$. This difference is a general statement of a lack of unique definition of the quark mass and for small m_q the differences become insignificant. At finite m_q we incorporate this non-uniqueness through the factor $f \equiv \partial m_q/\partial(2\kappa)^{-1}$ as is relevant in the case of F and D parameters discussed below. In Table 2 we also list the value of κ_s corresponding to the strange quark. It is roughly the relevant scale below which measurable effects of vacuum polarization are expected to show up.

β	κ_s	κ_c	β^κ_{eff}	a^{-1} GeV	β^a_{eff}
5.3	0.167	0.1685	5.71	1.2	
5.4	0.163	0.16437	5.78	1.60	5.75
5.5	0.160	0.16147	5.86	1.93	5.88
5.6	0.1572	0.15815	5.96	2.40	6.04

Table 2: The lattice scale a^{-1} and κ_c for the dynamical runs. We also list the effective quenched couplings with the same critical parameters.

5. Spectrum using Smeared Quark Propagators: We use periodic boundary conditions for both the gauge and fermion action in the update. The calculation of quark propagators is done on doubled lattices *i.e.* $16^3 \times 16 \rightarrow 16^3 \times 32$. We use the Wuppertal source method to calculate smeared quark propagators and to build hadron correlators out of these [6]. In almost all cases the smearing radius is ≈ 4 lattice units. In addition to smearing the source, one can also smear the sink point. This gives us two different constructions of the hadron correlators and we compare their efficacy in yielding asymptotic results. We find that both methods give results within errors though in general the effective mass reaches a plateau one time slice earlier with correlators smeared at both ends. On the other hand, the fluctuations in the effective mass are usually larger with the doubly smeared correlators. Thus, while smearing improves the overlap with the hadronic state it also increases noise due to fluctuations in the gauge links on the smeared time slice. Optimization, therefore, has to be done with respect to these two factors. We find it worthwhile calculating correlators with and without smearing at the sink time slice because the two numbers provide a consistency check while the extra CPU time is a tiny fraction overall.

Fig 3: APE plot using data given in Table 3.

The mass of the lowest state is extracted from the hadron correlators using the following procedure: for each state we first examine the single mass effective plot for the existence of a stable plateau and then make a single mass fit over this range of the plateau using the full covariance matrix to minimize χ^2. The errors in the fit parameters are calculated using the single elimination jackknife method.

The final results for the π, ρ, nucleon and the Δ are given in Table 3, along with the extrapolated

values assuming that m is linear in $1/\kappa$ for channels other than the pion. The table also lists values for $Z_A^{-1} f_\pi$ (normalized such that the experimental value is $f_\pi = 132\ MeV$) [4]. The data show the desired trend: the ratio m_N/m_ρ decreases while m_Δ/m_N increases as the quark mass is decreased.

Finally, the above data are presented on an APE plot in Fig. 3. The lightest quark mass is roughly m_s and for such heavy quarks one gets results that are very similar to those found in quenched simulations and consistent with phenomenological models. I consider this agreement to indicate that the dynamical update is working on lattices as large as $16^3 \times 32$ and for $m_q \approx m_s$.

6. SU(3) Mass Splittings and the F and D Parameters: for the symmetry breaking mass term $\frac{1}{\sqrt{3}}(m - m_s)\ \bar{q}\lambda_8 q$, where $m = m_u = m_d$ and $\mathrm{Tr}\lambda_a\lambda_b = 2\delta_{ab}$, the first order SU(3) mass splittings are characterized by the matrix elements of the three scalar densities $A \equiv \langle P|\bar{u}u|P\rangle$, $B \equiv \langle P|\bar{d}d|P\rangle$ and $C \equiv \langle P|\bar{s}s|P\rangle$. $|P\rangle$ is in general any hadronic state although we will mainly be concerned with the proton.

The mass splittings within the baryon octet can be parameterized in terms of the two reduced matrix elements F_S and D_S for a symmetry breaking term that transforms as λ_8. These parameters can be expressed in terms of matrix elements of the scalar densities: $2F_S = (A - C)$ and $2D_S = (A - 2B + C)$ and experimental data yields

$$\begin{aligned} 2F(m_s - m) &= M_\Xi - M_P &&= 0.379\ GeV \\ 2D(m_s - m) &= M_\Xi + M_P - 2M_\Sigma &&= -0.129\ GeV \\ 2D(m_s - m) &= 0.5(M_\Lambda - M_\Sigma) &&= -0.116\ GeV \end{aligned}$$

Knowing $(m_s - m)$ one can predict F and D and *vice versa*. In the limit of infinitely heavy quarks $F = 1$ and $D = 0$; deviations from these values arises due to the relativistic motion of the quarks. Lattice calculations allow us to map the interval between $m_q = \infty$ and the physical value of m_q [7].

We calculate the valence contribution to A and B using the ratio $\mathcal{R}$ of the 3-point (insertions on the valence quarks only) to the 2-point correlation functions. The long time behavior of such ratios with either scalar or axial vector insertions is for example

$$0.5\ R_u^S(t) \stackrel{t\to\infty}{\longrightarrow} const.\ + f\ \frac{F_S}{Z_S^L}\ t\ .$$

We have set $C = 0$ in which case $2F = A$. (This is also true in the limit of SU(3) symmetry as then the sea contributions cancel). We find a good signal using smeared operators for both A and B while that for the combination $2D = A - 2B$ is much more noisy. The final results are given in Table 4 along with the value for A in the ρ^+ and Δ^{++}. The gross features in the data are that the value of F does not change much as the quark mass is decreased from $3m_s$ to m_s while the magnitude of D increases as expected. A fit to all the data would suggest $m_s - m \approx 170\ MeV$.

To make comparison with the quenched theory, we have analyzed $16^3 \times 40$ lattices at $\beta = 6.0$ and $\kappa = 0.154$ and 0.155. The results at $\kappa = 0.154$ $(m_q \approx m_s)$ are indistinguishable within the statistical errors from those in Table 4. We find that the quenched values increase by $\approx 20\%$ between $\kappa = 0.154$ and 0.155.

	F_S	D_S	ρ_S	Δ_S
$m_q = \infty$	1	0	1	3
Expt.	$190/m_{SB}$	$-61/m_{SB}$	$124/m_{SB}$	$440/m_{SB}$
κ_v	fF_S/Z_S	fD_S/Z_S	$f\rho_S/Z_S$	$f\Delta_S/Z_S$
.162	1.03(7)	−0.13(11)	0.74(7)	2.5(2)
.158	0.90(6)	−0.05(5)	0.89(10)	2.5(2)
.159	1.12(7)	−0.12(6)	0.86(7)	2.6(3)
.160	0.99(6)	−0.28(6)	0.74(8)	2.0(3)
.156	1.03(7)	−0.11(4)	0.90(5)	2.5(2)
.157	1.10(6)	−0.17(5)	1.08(9)	3.3(4)

Table 4: Non-singlet scalar density matrix elements. The experimental numbers are extracted assuming first order symmetry breaking through the mass term $m_{SB} = m_s - (m_u + m_d)/2$ in MeV.

7. Pion-nucleon Sigma Term: Neglecting C, the pion-nucleon sigma term is given by

$$\Sigma^{val}_{\pi NN} = \bar{m}\langle P|\bar{u}u + \bar{d}d|P\rangle = \bar{m}(3F - D) \ .$$

Using $F \approx 1.05$, the phenomenologically derived value $D/F \approx -0.32$ and $\bar{m} \approx 7\ MeV$, we arrive at the canonical value $\Sigma^{val}_{\pi NN} = 3.5\bar{m} = 25\ MeV$.

The combination $A + B$ can also be calculated from the numerical derivative $\partial M_P/\partial m_q$. Note that on lattices with dynamical fermions, this method gives $\Sigma^{val}_{\pi NN} + \Sigma^{sea}_{\pi NN}$. Thus the difference in value between the derivative method and that derived from R gives $\Sigma^{sea}_{\pi NN}$. Our data at $\beta = 5.5$ and 5.6 yields the rough estimate $\Sigma = 9(2)\bar{m}$ at $m_q \sim m_s$. Even though the errors are large and most likely underestimated (we have ignored the dependence on m_q; the data indicates that $\Sigma/\bar{m}$ increases as $m_q \to 0$), this result favors a large sea quark contribution *i.e.* $\Sigma^{sea}_{\pi NN} \sim \Sigma^{val}_{\pi NN}$. We find, as required for consistency, that the derivative of the proton data obtained in the quenched approximation at $\beta = 6.0$ gives $\Sigma^{val} \sim 3.7\bar{m}$.

We find a similar behavior in the ρ and the Δ channels *i.e.* $A^{sea} \approx A^{val}$. Furthermore, the magnitude of the matrix element is roughly proportional to the number of valence quarks and is otherwise independent of the hadronic state. This suggests a model for constituent quarks in which, to zeroth approximation, the dressing is independent of the hadronic state and has a large sea contribution.

8. Non-singlet axial vector couplings F_A and D_A: Experimental results for the $SU(3)$ reduced matrix elements of the axial current for the proton, F_A and D_A, come from the spin correlations and lifetime of neutron decay $g_A = F_A + D_A = 1.259(4)$, and from a fit to all the semi-leptonic hyperon decay rates $F_A/D_A = 0.59(5)$. Using the non-relativistic quark model, the results in the static ($m_q = \infty$) limit are $g_A = 5/3$ and $F_A/D_A = 2/3$.

κ	0.162	0.158	0.159	0.160	0.156	0.157
fF_A/Z_A	.52(5)	.57(2)	.59(3)	.53(5)	.56(2)	.57(3)
fD_A/Z_A	.83(3)	.86(2)	.86(2)	.84(4)	.86(2)	.88(3)

Table 5: Non-singlet axial current matrix elements of the proton. The experimental values are $F_A = 0.48$ and $D_A = 0.78$.

We find a reasonable signal for both F_A and D_A and the data (Table 5) do not show any statistically significant variation with β or m_q. The results are consistent with the experimental numbers if we use $f \sim 0.97$ and $Z_A \sim 0.85$. The quenched results at $\beta = 6.0$ and $\kappa = 0.154$ are similar to those in Table 5 and show a $\sim 10\%$ decrease as κ is increased to 0.155.

Acknowledgements: We are grateful to ACL at LANL, PSC, TMC, NPAC, Sandia, SDSC and Argonne for the tremendous support received for these calculations.

REFERENCES

1. S. Duane, A.Kennedy, B.Pendleton, D.Roweth, *Phys. Lett.* **195B** (1987) 216.
2. R. Gupta, A. Patel, C. Baillie, G. Guralnik, G. Kilcup and S. Sharpe, *Phys. Rev.* **D40** (1989) 2072.
3. R. Brickner, these proceedings.
4. D. Daniel, R. Gupta, D. Richards, LA-UR-90-3469.
5. R. Gupta, G. Kilcup and S. Sharpe, *Phys. Rev.* **D38** (1988) 1288.
6. S. Güsken, *Nucl. Phys.* **B** (*Proc. Suppl.*) **17** (1990) 361.
7. L. Maiani, G. Martinelli, M. Paciello, B. Taglienti, *Nucl. Phys.* **B293** (1987) 420
   R. Sommer *Nucl. Phys.* **B** (*Proc. Suppl.*) **17** (1990) 513.

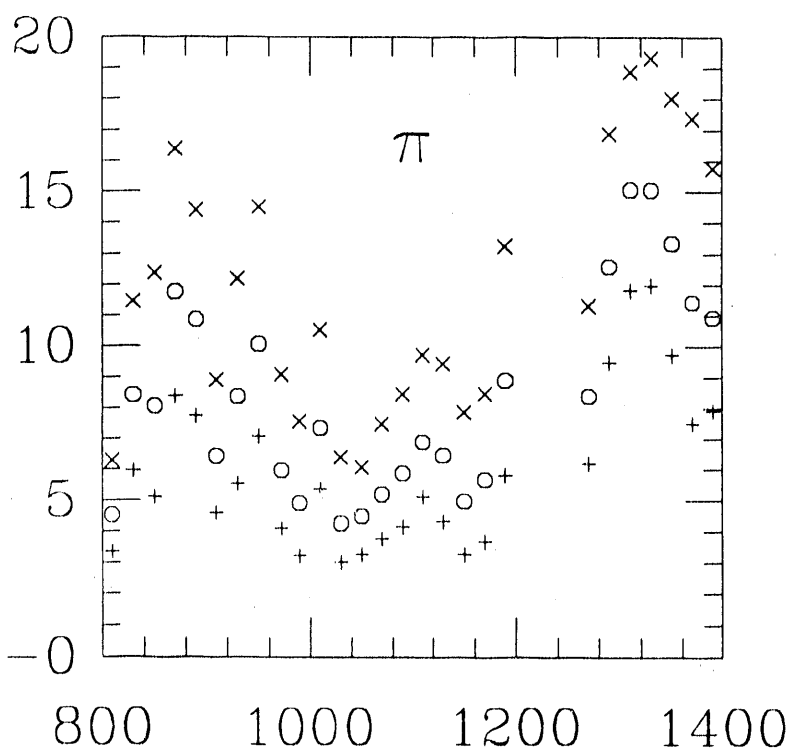
20
15
10
5
0
π
800
1000
1200
1400

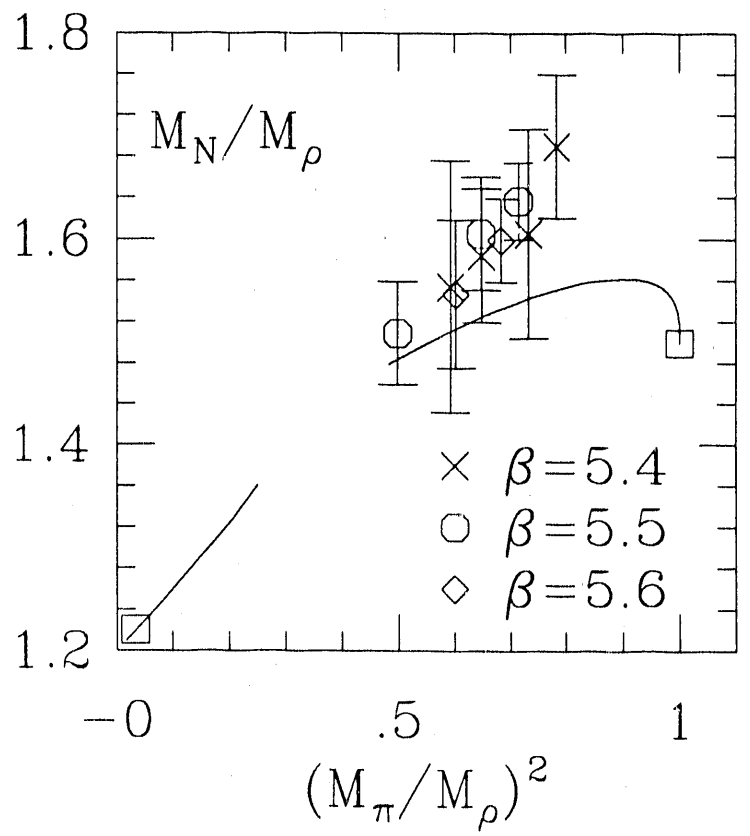
1.8
1.6
1.4
1.2
M_N/M_ρ
× β=5.4
○ β=5.5
◇ β=5.6
−0
.5
1
$(M_\pi/M_\rho)^2$

β	κ	N_l	π	$Z_A^{-1} f_\pi$	ρ	N	Δ	N/ρ	Δ/N
5.4	.160	15	0.77(2)	0.21(1)	0.87(2)	1.47(5)	1.54(10)	1.69(07)	1.05(08)
5.4	.161	15	0.65(2)	0.18(2)	0.76(2)	1.22(7)	1.27(10)	1.61(10)	1.04(10)
5.4	.162	14	0.569(11)	0.16(1)	0.71(1)	1.12(4)	1.22(5)	1.58(07)	1.09(05)
5.4	.163	4	0.43		0.56	0.86	0.93	1.54	1.08
5.4	.16437				0.48	0.68	0.86		
5.5	.158	15	0.568(5)	0.15(1)	0.672(9)	1.10(2)	1.17(3)	1.64(04)	1.06(03)
5.5	.159	17	0.481(5)	0.13(1)	0.598(8)	0.96(3)	1.05(3)	1.61(05)	1.09(05)
5.5	.160	27	0.365(12)	0.114(5)	0.517(11)	0.78(2)	0.89(3)	1.51(05)	1.14(05)
5.5	.16147				0.40	0.55	0.69		
5.6	.156	16	0.486(7)	0.125(6)	0.588(8)	0.94(2)	1.00(3)	1.60(04)	1.06(04)
5.6	.157	35	0.352(6)	0.102(4)	0.459(9)	0.71(2)	0.78(3)	1.55(07)	1.10(06)
5.6	.15815				0.32	0.45	0.533		

Table 3: Meson and baryon spectrum using N_l lattices for the different parameters given in table 1.

END

DATE FILMED

01 / 16 / 91